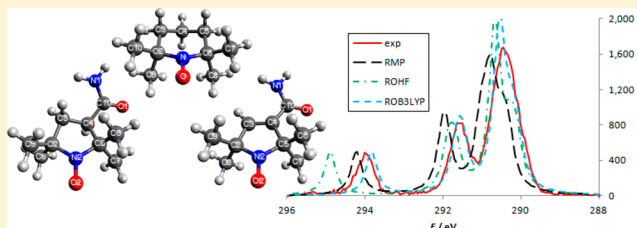


# Reliability of Density Functional and Perturbation Theories for Calculating Core-Ionization Spectra of Free Radicals

Ivan Ljubić\*

Department of Physical Chemistry, Ruđer Bošković Institute, Bijenička Cesta 54, HR-10000 Zagreb, Croatia

**ABSTRACT:** The C 1s, N 1s, and O 1s ionization energies were calculated for the three stable nitroxide free radicals, viz., tempo and its two analogues, and compared to their most recent high-resolution core photoelectron spectra. We compare the performance of unrestricted and restricted open shell based  $\Delta$ HF,  $\Delta$ MP2, and  $\Delta$ B3LYP methods. A mixed basis set is employed in all cases, which consists of the core–valence correlation-consistent triple- $\zeta$  basis set (cc-pCVTZ or cc-pwCVTZ) on the atom whose core–electron binding energy is calculated, model core potentials on the remaining first row atoms, and the cc-pVDZ basis set on the hydrogen atoms. The best overall performance for the three free radicals is offered by the restricted open shell based  $\Delta$ B3LYP method. Surprisingly, both the restricted open and unrestricted second-order perturbation theories perform relatively poorly and typically do not warrant additional computational effort over the reference  $\Delta$ HF methods. This is particularly true of the  $\Delta$ ZAPT method, which exhibits a number of grave failures that render it unsuitable for calculating the core-ionization spectra.



## I. INTRODUCTION

The past several decades have seen remarkable progress in spectroscopic techniques that have in common exciting and/or ejecting of electrons from the innermost (core) orbitals of atoms or molecules, followed by acquisition and interpretation of data on the core electron binding energies (CEBEs), current, and angular distribution.<sup>1</sup> Numerous refinements have increasingly established the techniques such as X-ray photoelectron spectroscopy (XPS), X-ray absorption (XAS), X-ray emission spectroscopy (XES), and others, as powerful probes of molecular properties and dynamics equally applicable in solid, liquid, and gas phases. Nowadays sources of high energy, intensity, and coherence routinely provide a fine enough resolution of energy shifts to reveal highly sensitive information on local properties of core-ionized atoms such as atomic charge, valence, hybridization, electronegativity, proton affinity, and the nature of the chemical bonds.<sup>2</sup> These data are in turn frequently specific enough to allow for an unambiguous determination of not merely the raw chemical composition of the sample but also of its structural formula and, e.g., fine vibrational structure.<sup>3</sup>

Most recently, the gas-phase core-ionization XPS spectra of the three stable doublet nitroxide free radicals, tempo, nitroxyl8, and nitroxyl9, were recorded (Figure 1; the labeling for the latter two compounds follows that of ref 4).<sup>5</sup> The experimental and theoretical data indicated that the unpaired spin density is located primarily on the oxygen atom of the nitroxide group,<sup>5</sup> which is attached to the piperidine (tempo), pyrrolidine (nitroxyl8), or azacyclopentene (nitroxyl9) ring. The radical center is protected and stabilized by the double methyl substitutions at the two vicinal carbon positions. The practical interest in spectroscopic properties and the chemistry of stable nitroxide free radicals has been considerable ever since

1960 when the prototype molecule tempo was synthesized. These radicals have thus far found multiple uses in biology, medicine, and organic synthesis, notably as spin-labels in electron spin resonance spectroscopy, contrast agents in magnetic resonance imaging, probes for monitoring intracellular redox reactions, catalysts in green oxidations, and redox mediators in free radical polymerizations.<sup>6</sup> Apart from the practical interest, there is also a strong fundamental interest in modeling and interpreting the core-ionization spectra of free radicals. The CEBEs of the relevant atoms are capable of revealing valuable information about the nature of the radical centers, extent of (de)localization of the unpaired spin, and role of the adjacent atoms, while coupling of the unpaired core and valence electrons in the core hole cations is expected to enrich the spectra with additional features.<sup>5</sup>

Accurately predicting, preferably to within 0.2 eV, CEBEs in atoms or molecules by quantum chemical methods remains challenging. The predominantly pursued approach, generally denoted by  $\Delta$ SCF (SCF = self-consistent field), consists of explicitly converging the ground and core-ionized state densities and subsequently taking their energy difference to obtain the CEBE. Such a simple procedure is readily applicable in the context of (post-)Hartree–Fock (e.g.,  $\Delta$ HF,  $\Delta$ MP2,  $\Delta$ CCSD) or density functional theory ( $\Delta$ DFT) based methods. However, this logical approach to allowing for the relaxation of the initial and final states is frequently found to be prone to severe difficulties in achieving the convergence for the core hole state. In addition to the persistent risk of collapse of the delicate local core hole minimum, also challenging is localizing the half-filled core orbital unambiguously to the atom of interest to

Received: February 11, 2014

Published: May 8, 2014



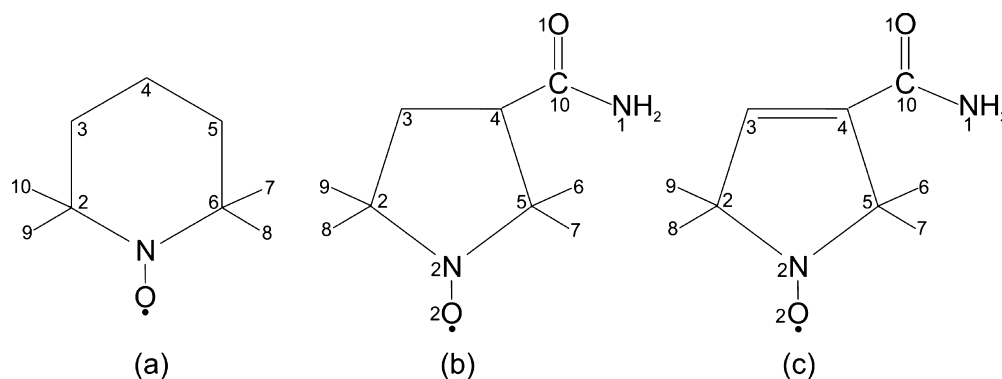


**Figure 1.** Three nitroxide radicals: (a) tempo ( $C_s$  symmetry), (b) nitroxyl8, and (c) nitroxyl9.

prevent the oscillatory behavior of the SCF procedure caused by shifting of the core hole among atoms of the same kind. Examples of approaches to preserving the desired core hole structure of the wave function are an intermediate optimization with the frozen core orbital in order to gradually advance to the radius of the core hole convergence,<sup>7</sup> and the maximum overlap method (MOM).<sup>8</sup> The unphysical delocalization of the core hole over symmetry-equivalent atoms,<sup>9</sup> which could here be the issue with the  $C_s$  symmetric tempo (Figure 1), is known to pose difficulties if symmetrized molecular orbitals are used.<sup>10</sup> To solve it, different ways of inducing breaking of the wave function symmetry were devised with good results for calculating CEBEs and X-ray absorption spectra.<sup>8,10</sup> The approach of using rescaled (one-electron) effective core potentials on core-ionized atoms was also tested in conjunction with a number of correlated treatments, up to  $\Delta\text{CCSD(T)}$ .<sup>11</sup>

Here we adopt a conceptually simple yet promising alternative, which solves the problem of localization of core hole by resorting to mixed basis sets, specifically an all-electron core–valence correlation basis set exclusively on the atom of interest and core potentials plus a set of  $d$  polarization functions on the remaining first row atoms.<sup>12</sup> This strategy ensures that the only core orbital present is the one on the atom whose CEBE is calculated in a given run while use of the comparatively economical basis sets on the remaining atoms both alleviates the convergence and provides an inexpensive alternative to the more commonly applied extensive all-electron basis sets used equally on all atoms.<sup>8</sup> Within the mixed basis set framework, restricted open shell  $\Delta\text{MP2}$  method in conjunction with the mixed basis set framework was calibrated on a test set of a number of closed shell molecules, up to nucleobases, resulting for the most part in CEBEs within 0.2 eV of the experimental values.<sup>12</sup> Thus, treating the core-ionized atom more elaborately than the rest of the system seemingly allows for an efficient treatment of larger systems without significant loss of accuracy.

Presently, two of the most popular ROHF based perturbation theories to the second order will be tested: (i) the restricted Møller–Plesset theory (RMP) of Knowles et al. and Lauderdale et al.,<sup>13</sup> and (ii) the  $Z$ -averaged perturbation theory (ZAPT) of Lee and Jayatilaka.<sup>14</sup> Starting from the converged ROHF wave function, the key difference between the RMP and ZAPT theories is in the re-definition of the orbitals and the corresponding orbital energies, which are subsequently used in constructing the zero-order Hamiltonian for the MP theory. The RMP theory requires the *semicanonical spin orbitals*,<sup>13</sup> whose definition results in each of the  $\alpha$ - and  $\beta$ -

spin–orbitals assuming its own distinct spatial part. The semicanonical spin orbitals can be thus thought of as UHF-like as it is possible to still retain the total spin as a good quantum number. Notwithstanding this, the computational burden of RMP can be reduced significantly relative to that of the standard UMP2 by taking advantage of the spin contamination restriction, which nominally leads to the  $\beta$ -occupied spatial parts spanning just the subspace of the  $\alpha$ -occupied spatial parts.<sup>13a</sup> The ZAPT method, on the other hand, uses the so-called *symmetric spin–orbitals*,<sup>15</sup> which retain the identical spatial parts and  $S_z$  eigenfunctions for the pairs of doubly occupied and unoccupied  $\alpha$ - and  $\beta$ -spin–orbitals. Characteristic, however, is the distinction between occupied and unoccupied parts of the open shell orbitals, which are assigned the  $\sigma^+$  and  $\sigma^-$   $S_x$  eigenfunctions, respectively, and thus formally attain different energies  $\epsilon^+$  and  $\epsilon^-$ . The reference wave function is thus “ $Z$ -averaged” in the sense of being a linear combination of all possible  $M_s$  states. Owing to the use of the symmetric spin–orbitals, ZAPT has computational costs similar to the closed shell MP2 and is particularly amenable to parallelization and efficient implementation of the analytical gradients.<sup>14</sup> The current credo is that the two ROHF based perturbation theories yield mostly similar results, which are indeed usually in favor of ZAPT when the differences between the two do become noteworthy.<sup>14b,16</sup>

As a computationally more efficient alternative, yet expectedly on par with the  $\Delta\text{MP2}$  treatments with regard to accuracy, the  $\Delta\text{DFT}$  methods have repeatedly been found to exhibit good performance in calculating absolute CEBEs, intra-molecular relative CEBEs (chemical shifts), and core-excited spectra of closed shell molecules.<sup>8,10,17,18</sup> In this setting, the unrestricted  $\Delta\text{B3LYP}$  approach was previously demonstrated to outperform both  $\Delta\text{UHF}$  and  $\Delta\text{UMP2}$ .<sup>8b</sup> Most recently, extensive comparative tests of the unrestricted  $\Delta\text{DFT}$  method employing a number of standard pure and hybrid GGA functionals were carried out.<sup>18</sup> Of the hybrid GGAs, B3PW91 was found to perform best. Interestingly, the B3LYP hybrid functional in the “B3LYP5” variant, which is the one to be used presently (vide infra), significantly outperformed the more widely used B3LYP variant.<sup>18</sup>

The goal of the present study is to assess the reliability of unrestricted (U) and restricted open (RO) shell  $\Delta\text{HF}$ ,  $\Delta\text{MP2}$ , and  $\Delta\text{DFT}$  approaches for predicting the gas-phase core hole spectra of the three nitroxide radicals. Because comparatively large species are involved, mixed all electron/core potentials basis sets will be employed for the reasons of improved runtime and convergence efficiency. Presently, both the ground state

and the core hole cation are open shell systems; thus, it is of interest to see whether restriction on the total spin as a good quantum number innate to the RO framework increases accuracy of the calculated CEBEs. The spin contamination in the unrestricted approaches may pose problems, more so for the UHF based correlation treatments than for U-DFT. In difficult cases this manifests in poor energies and spin densities, and in particular slow convergence of the SCF UHF problem and the MP series built on the spin contaminated UHF references.<sup>19</sup> On the other hand the restricted open shell SCF problem is itself often affected by slow and erratic convergence due to the rigorous constraints on the molecular orbitals. Thus, apart from the relative accuracy, comparing the feasibility of the U and RO theories with respect to the rate of SCF convergence to the challenging core hole states is also of interest.

## II. COMPUTATIONAL DETAILS

The CEBEs of the three nitroxyl radicals (Figure 1) are calculated using the unrestricted and restricted open shell based  $\Delta$ HF,  $\Delta$ MP2 and  $\Delta$ B3LYP approaches. The second-order perturbation corrections based on the restricted open shell HF references are calculated according to  $\Delta$ RMP<sup>13</sup> and  $\Delta$ ZAPT<sup>14</sup>. In line with the original study,<sup>12</sup> on the atom whose CEBE is calculated in a given run, we use the correlation-consistent triple- $\zeta$  basis set augmented with tight s, p, and d functions for the description of the core–core and core–valence electron correlation (cc-pCVTZ).<sup>20</sup> However, we also test the more recent weighted variant (cc-pwCVTZ)<sup>21</sup> because it is considered an improvement over the original cc-pCVTZ basis, especially with regard to the better description of the core–valence (intershell) correlation effects which tend to be more important for the energetics.<sup>21</sup> For the remaining C, O, and N atoms the model core potentials (MCP) are used with a double- $\zeta$  contraction and a set of d polarization functions in the valence space (MCP-dzp) as devised by Miyoshi and co-workers.<sup>22</sup> The standard correlation-consistent double- $\zeta$  basis set (cc-pVDZ) is used on all hydrogen atoms.<sup>23</sup> The described mixed basis sets are designated as CV (wCV) to distinguish between the cc-pCVTZ (cc-pwCVTZ) basis sets used on the core-ionized atom. Because the core-correlating basis functions are included in the CV and wCV sets, none of the orbitals was kept frozen in calculating the second-order correction to energy. Only the high-spin (triplet) multiplicity is considered for the core hole cations. For the  $\Delta$ DFT calculations, the hybrid B3LYP<sup>24</sup> exchange–correlation functional was used with the parametrization as implemented in the GAMESS-US program.<sup>25</sup> This parametrization specifically concerns the choice of the fifth formula from the study by Vosko, Wilk, and Nusair on the correlation in electron gas.<sup>26</sup> The equilibrium geometries of the three radicals were optimized at the U-B3LYP/6-31+G(d) level, which should be adequate because CEBEs were observed to be largely insensitive to the small differences in the geometric parameters.<sup>12</sup> This was checked for several atoms by employing the UMP2/6-31+G(d) optimized geometry instead, which predicts the analogous conformations but has on average 0.01 Å shorter bonds. The deviations of this size indeed brought about only very small differences in the CEBEs, on the order of 0.01–0.03 eV. The unchanged U-B3LYP ground state geometries were also assumed for the core hole cations. The GAMESS-US quantum chemical software was used in all calculations.<sup>25</sup>

**A. Convergence Properties of the RO- and U-Theories.** Achieving the restricted open shell SCF convergence proved

difficult for most of the atoms, most notably for O2, N atoms, and the C atoms of the CH<sub>3</sub> substituents (Figure 1). To preserve the desired core hole configuration, the mixings of occupied and virtual orbitals and the orbital interchanges need to be restricted (the RSTRCT flag in GAMESS-US). This maintains a maximum overlap between the initial core hole orbital guess assembled from the ground state orbitals and the orbitals in subsequent SCF iterations similarly to the MOM approach.<sup>8</sup> In all cases the default second-order SCF (SOSCF) procedure had to be abandoned in favor of the Pulay's DIIS convergence accelerator.<sup>27</sup> In addition, occasionally the default dimension (9) of the DIIS iterative subspace had to be reduced significantly to advance toward the solution. Dynamically interchanging the DIIS with the Pople extrapolation of the (previous three) Fock matrices proved crucial for achieving the RO-B3LYP convergence on several instances. The cumbersome oscillatory behavior of the energy during the SCF iterations forced us to frequently restart the SCF procedure, each time manually providing a hopefully better initial guess of the density to converge only very slowly and erratically to the targeted core hole solution. The starting densities were gradually improved by adopting a trial-and-error procedure which entailed estimating which one from the collection of previous SCF iterations might result in the most favorable guess of the density for the restarted SCF procedure; here, importantly, the commonsense lowest energy criterion more often than not proved misleading. In general, the described strategy of achieving the ROHF SCF convergence for the core hole wave functions of the molecules of this size proved far from a ready-made procedure and requires some experience and patience. Importantly, however, the described pronounced convergence difficulties with the three nitroxyl radicals were entirely unlike tests on a number of smaller molecules that were conducted beforehand (up to CH<sub>3</sub>COOCH<sub>3</sub>), none of which exhibited difficult convergence. Accordingly, the convergence of the core hole (and presumably core-excited) wave functions within the restricted open shell SCF framework becomes more of an issue with the increasing number of basis functions. In addition, in the specific case of the core hole states of the three radicals, the valence singly occupied orbital persistently oscillates between the correct  $\pi^*(\text{N}=\text{O})$  and several of the near-lying bonding orbitals. This frequent flipping exacerbates the convergence further. For the restricted open B3LYP, the SCF convergence was even more cumbersome than for the ROHF, especially for the N and O atoms.

On the other hand, for the unrestricted theories, while we did encounter some convergence issues, these were never as serious as with the ROHF/RODFT. This makes the unrestricted calculations considerably less time-consuming than their RO counterparts. Here the desired core hole configuration can be preserved practically equally efficiently either through the use of the MOM algorithm<sup>8</sup> (in GAMESS-US this is available for the unrestricted but not for the restricted open shell theories) or by restricting the orbital rotations (RSTRCT). Thus, from the standpoint of convergence properties and the corresponding time savings, the unrestricted approaches to calculating CEBEs of the free radicals enjoy a significant comparative advantage.

**B. Comparing the Experimental and Theoretical Data.** The C 1s core-ionization spectra exhibit complex overlapping bands corresponding to the nine C atoms, all of which are inequivalent in nitroxyl8 and nitroxyl9. Consequently, the accurate experimental data, specifically the positions of the vertical core-ionization energies as well as the assignment of a

**Table 1.** C 1s, N 1s, and O 1s Core-Electron Binding Energies (eV) of the Three Nitroxide Radicals (Figure 1) Calculated with Restricted Open Shell Methods. ( $\Omega_{\text{rel}}$  = Relative Overlap between the Experimental and Modeled C 1s Spectra; AAD = Average Absolute Deviation)

atom	$\Delta\text{ROHF wCV}$	$\Delta\text{ZAPT}^a \text{ CV}$	$\Delta\text{RMP CV}$	$\Delta\text{RMP wCV}$	$\Delta\text{RO-B3LYP wCV}$	exp
Tempo						
C2=C6	291.35	291.78	291.68	291.65	291.27	291.3
C3=C5	290.43	291.17	290.22	290.74	290.43	290.4
C4	290.49	290.94	291.14	290.78	290.50	290.7
C7=C10	290.22	290.25	290.63	290.39	290.21	290.1
C8=C9	290.29	290.19	290.76	290.52	290.28	290.4
N	405.58	404.40	405.75	407.09	405.99	406.4
O	535.61	534.54	537.14	536.95	536.02	537.0
$\Omega_{\text{rel}}$	0.89	0.74	0.73	0.73	0.88	
Nitroxyl8						
C2	291.69	292.00	292.02	291.88	291.52	291.4
C3	290.97	292.69	291.25	291.16	290.83	290.7
C4	291.04	291.23	291.35	291.18	290.85	290.7
C5	291.57	291.92	291.91	291.77	291.38	291.4
C6	290.33	290.52	290.74	290.52	290.28	290.1
C7	290.16	290.15	290.04	290.31	290.12	290.1
C8	290.59	289.36	290.99	290.76	290.53	290.4
C9	290.60	290.19	290.94	290.71	290.52	290.4
C10	294.76	294.03	294.24	294.11	293.78	293.8
N1	405.97	406.05	406.35	406.40	405.87	405.9
N2	405.73	408.52	409.88	407.23	406.08	406.4
O1	536.07	537.34	537.29	537.10	536.33	536.8
O2	535.90	537.43	537.38	537.19	536.25	537.2
$\Omega_{\text{rel}}$	0.75	0.61	0.63	0.72	0.88	
Nitroxyl9						
C2	291.87	292.15	292.15	292.02	291.65	291.6
C3	290.70	291.17	290.70	290.91	290.49	290.7
C4	290.70	290.99	291.22	291.06	290.62	290.7
C5	291.69	292.03	292.06	291.91	291.50	291.6
C6	290.29	290.01	290.72	290.49	290.26	290.1
C7	290.12	290.14	290.54	290.33	290.10	290.5
C8	290.61	280.48	290.95	290.73	290.52	290.5
C9	290.66	288.45	291.00	290.78	290.57	290.5
C10	294.90	294.45	294.36	294.22	293.84	294.0
N1	405.94	406.35	406.26	406.32	405.80	405.9
N2	405.85	407.70	407.21	407.28	406.19	406.7
O1	536.11	537.39	537.34	537.16	536.30	536.9
O2	536.02	537.54	537.48	537.29	536.36	537.3
$\Omega_{\text{rel}}$	0.75	0.52	0.59	0.68	0.89	
AAD	0.40	0.96	0.51	0.33	0.24	

<sup>a</sup>When applicable, only the rectified  $\Delta\text{ZAPT}$  results are given (details in the text).

detailed relative ordering to the C atoms, was rather difficult to infer from the comparative empirical analysis of the spectra.<sup>5</sup> Thus, simply considering the average absolute deviation (AAD) between the theoretical and experimental vertical CEBEs is not guaranteed to give a best impression of the performance of the theoretical treatments because only a moderately accurate set of vertical CEBEs could be extracted from the spectra.<sup>5</sup> For this reason, it is reasonable to define an alternative measure of agreement between the experiment and theory as the overlap  $\Omega$  between the experimental ( $f_{\text{exp}}$ ) and modeled ( $f_{\text{theor}}$ ) spectral curves:

$$\Omega = \int \min(f_{\text{theor}}(E), f_{\text{exp}}(E)) dE \quad (1)$$

The integration in eq 1 extends over the entire spectral range. The spectra are modeled by using Lorentzian line shapes

centered at the predicted values of CEBEs. These simple line shapes are sufficiently accurate for the present purpose, as seen by, e.g., the nice overlap between the Lorentzian and the well-resolved peak at  $\sim 294$  eV (e.g., Figure 4). The area under the modeled spectral curve is always normalized to the area under the corresponding experimental curve. Hence it is useful to define the relative overlap ranging from 0 (null agreement) to 1 (perfect agreement) as

$$\Omega_{\text{rel}} = \frac{\Omega}{\int f_{\text{exp}}(E) dE} \quad (2)$$

The only remaining free parameter, the full width at half-maximum, specifies the line width of the Lorentzians. This was kept constant at 0.35 eV ( $\sim 2800 \text{ cm}^{-1}$ ), common to all of the C atoms of the three radicals.



### III. RESULTS AND DISCUSSION

**A. Comparison to Experiment.** Tables 1 and 2 compile the CEBEs for the three nitroxide radicals shown in Figure 1.

**Table 2. C 1s, N 1s, and O 1s Core-Electron Binding Energies (eV) of the Three Nitroxide Radicals (Figure 1) Calculated with Unrestricted Methods. ( $\Omega_{\text{rel}}$  = Relative Overlap between the Experimental and Modeled Spectra (Details in the Text); AAD = Average Absolute Deviation)**

atom	$\Delta$ UHF wCV	$\Delta$ UMP2 wCV	$\Delta$ U-B3LYP wCV	exp
Tempo				
C2=C6	291.12	291.59	291.14	291.3
C3=C5	290.19	290.68	290.31	290.4
C4	290.25	290.70	290.38	290.7
C7=C10	289.97	290.31	290.08	290.1
C8=C9	290.04	290.43	290.16	290.4
N	406.29	408.28	405.83	406.4
O	535.38	536.79	535.85	537.0
$\Omega_{\text{rel}}$	0.67	0.81	0.77	
Nitroxyl8				
C2	291.47	291.82	291.40	291.4
C3	290.72	291.07	290.71	290.7
C4	290.79	291.48	290.73	290.7
C5	291.35	291.72	291.26	291.4
C6	290.09	290.42	290.16	290.1
C7	289.91	290.23	290.00	290.1
C8	290.35	290.66	290.41	290.4
C9	290.35	290.63	290.40	290.4
C10	294.41	294.80	294.23	293.8
N1	405.71	406.35	405.74	405.9
N2	405.49	407.04	405.92	406.4
O1	535.79	537.00	536.18	536.8
O2	535.66	537.01	536.09	537.2
$\Omega_{\text{rel}}$	0.83	0.72	0.87	
Nitroxyl9				
C2	291.63	292.15	291.53	291.6
C3	290.32	291.11	290.37	290.7
C4	290.36	291.13	290.49	290.7
C5	291.46	291.90	291.39	291.6
C6	290.04	290.38	290.14	290.1
C7	289.87	290.22	289.97	290.5
C8	290.36	290.74	290.40	290.5
C9	290.41	290.74	290.45	290.5
C10	294.71	294.19	294.08	294.0
N1	405.68	406.38	405.67	405.9
N2	405.61	407.02	406.03	406.7
O1	535.83	537.02	536.15	536.9
O2	535.79	537.18	536.20	537.3
$\Omega_{\text{rel}}$	0.76	0.70	0.85	
AAD	0.43	0.37	0.31	

The relative overlaps (for the C 1s spectra only) and AADs (calculated over all pairs of the experimental–theoretical values) are also reported in Tables 1 and 2. Figures 2–7 show the modeled C 1s core-ionization spectra superimposed on the experimental spectra from ref 5.

For the calculations of CEBEs we used the geometries of the three free radicals optimized at the UB3LYP/6-31+G(d) level. The influence of structural relaxation and vibrational effects on the spectra is presently not considered. The tempo radical assumes the  $C_s$  symmetric chair conformation, which was also obtained recently.<sup>28</sup> The most stable conformations assumed by

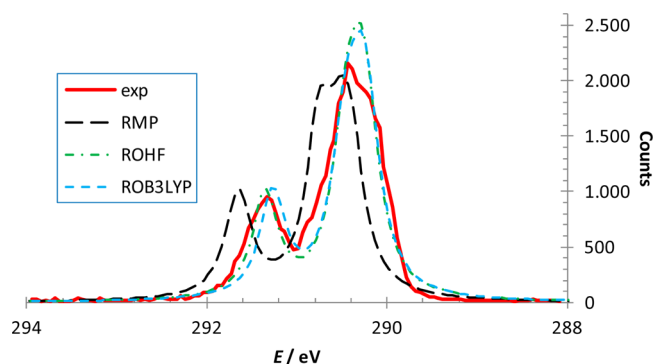


**Figure 2.** Experimental and modeled C 1s core-ionization spectra of tempo for the restricted open shell theories. The wCV mixed basis set is used.

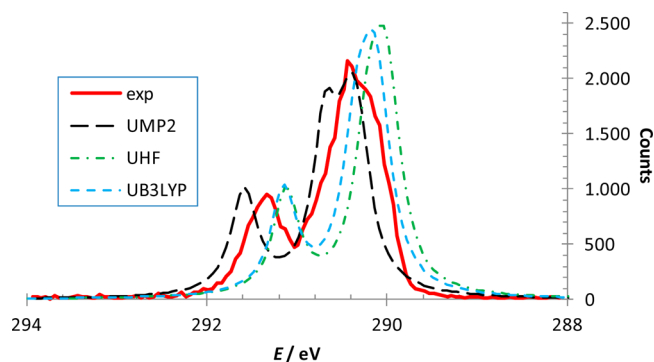


**Figure 3.** Experimental and modeled C 1s core-ionization spectra of tempo for the unrestricted theories. The wCV mixed basis set is used.

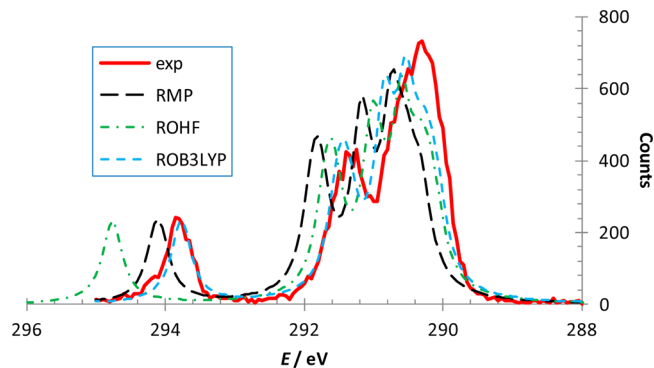


**Figure 4.** Experimental and modeled C 1s core-ionization spectra of nitroxyl8 for the restricted open shell theories. The wCV mixed basis set is used.

nitroxyl8 and nitroxyl9 reflect the increasing steric strains in the five-membered rings, which have to accommodate the bulky dimethyl and amide substituents in the vicinal position. The nitroxyl8 conformation is closest to a  $\text{CH}_2$ -tip envelope, which is slightly twisted (the C2–N2–C5–C4 dihedral angle is  $13^\circ$ ) to relieve the steric strain between the vicinal dimethyl and amide substituents. The nitroxyl9 ring is nearly planar with the C3–C2–N2–C5 dihedral angle equal to  $6^\circ$ . The possibility of the amide–iminol tautomerism can also be envisaged,<sup>29</sup> and despite this being enhanced due to the presence of the conjugated double bond in nitroxyl9, the effects on the spectra under experimental conditions should be entirely negligible; the zero point energies (ZPEs) corrected differences are 17.6 and

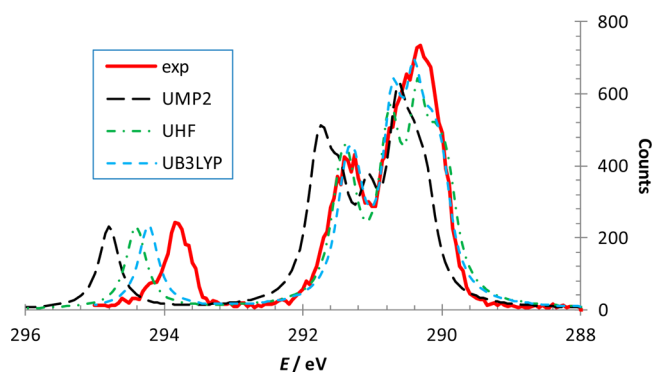


**Figure 5.** Experimental and modeled C 1s core-ionization spectra of nitroxyl8 for the unrestricted theories. The wCV mixed basis set is used.

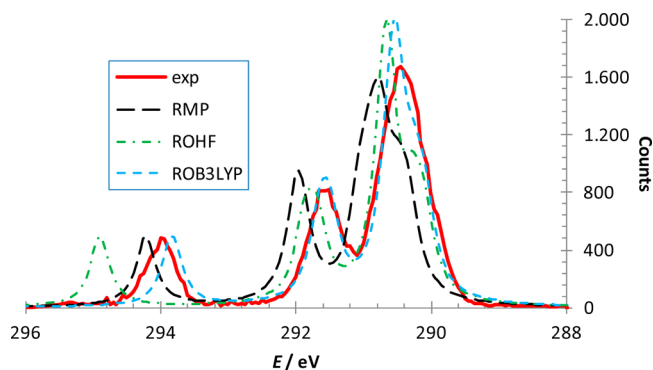


**Figure 6.** Experimental and modeled C 1s core-ionization spectra of nitroxyl9 for the restricted open shell theories. The wCV mixed basis set is used.

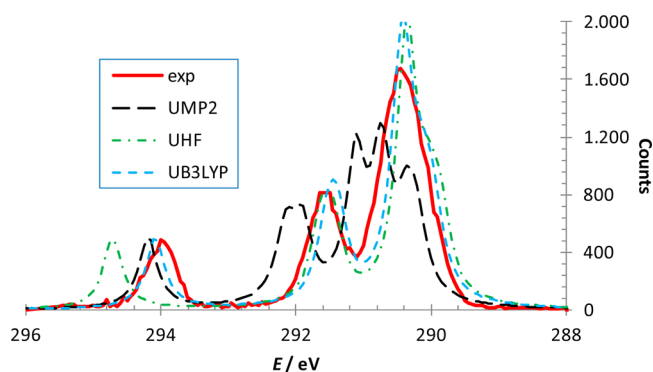


**Figure 7.** Experimental and modeled C 1s core-ionization spectra of nitroxyl9 for the unrestricted theories. The wCV mixed basis set is used.

14.6 kcal mol<sup>−1</sup> in favor of the amide structures in nitroxyl8 and nitroxyl9, respectively.

The C 1s core-ionization spectra are well-resolved into groups of two (tempo) or three (nitroxyl8 and nitroxyl9) bands.<sup>5</sup> These basic features are qualitatively reproduced by each of the tested methods (Figures 2–7). The most intense first band (~290–291 eV) comprises a majority of the absorptions, which are predicted to correspond to the ring C atoms and the four methyl substituents, with the exception of the C atoms attached directly to the nitroxyl group, which are contained in the second band (~291–292 eV). The third, most

blue-shifted, absorption (~294 eV) corresponds to the amide C atom.

In our previous study only the  $\Delta$ SCF/CV CEBEs were reported, the accuracy of which was sufficient to aid in resolving some of the ambiguities of the experimental assignment.<sup>5</sup> However, the most prominent discrepancy there concerned the overestimated O2 CEBEs for nitroxyl8 and nitroxyl9, which was rationalized in terms of the multiple close-lying local minima and difficulties in steering the volatile course of the SCF optimization to the correct minimum. Presently, however, we managed to converge to the lower core hole solution so that this particular CEBE for the O2 radical center does not appear as problematic any more (Tables 1 and 2). The  $\Delta$ SCF/CV O2 CEBEs are thereby also corrected to 535.94 (536.06 eV) for nitroxyl8 (nitroxyl9), and the overall AAD for the SCF/CV method is reduced to 0.43 eV from the originally reported 0.47 eV.<sup>5</sup>

We also tried to improve on the originally proposed  $\Delta$ RMP/CV method<sup>12,30</sup> by using the more recent cc-pwCVTZ in lieu of the cc-pCVTZ basis set on the core-ionized atom. This change was indeed found to be very beneficial for the  $\Delta$ RMP method (Table 1), while for the  $\Delta$ HF and  $\Delta$ DFT approaches the changes are virtually negligible so only the wCV values are reported. The largest improvement is seen for the N2 atom of nitroxyl8 where  $\Delta$ RMP/wCV succeeds in shifting the suspicious  $\Delta$ RMP/CV value considerably closer to the more reasonable CEBE calculated for the analogous atom in nitroxyl9. However, the potential for annoying unpredictable oscillations of the second-order treatments is illustrated by the N atom of tempo where despite similar values of the reference  $\Delta$ SCF/CV<sup>5</sup> and  $\Delta$ SCF/wCV energies a discrepancy of 1.34 eV is seen between the  $\Delta$ RMP/CV and  $\Delta$ RMP/wCV values (Table 1). The  $\Delta$ ZAPT approach exhibits intractable fundamental problems regardless of which of the two mixed basis set is used (section IIIB).

An accurate assignment of the 290–291 eV region proved difficult due to the complexity of the spectra and limited spectral resolution, which was for instance insufficient for resolving the fine vibrational structure in the simpler N 1s and O 1s spectra.<sup>5</sup> Consequently, the experimental errors are larger than those usually seen with the smaller closed shell molecules, such as those from a typical test set for the calibration of methods.<sup>8,12</sup> For this reason all of the experimental CEBEs are reported to only one decimal place (Tables 1 and 2). The comparison is presently made to the most intense of several of the Voigt profiles used in the reconstruction of the complex bands.<sup>5</sup> Due to relying on the linear coupling approximation,<sup>3</sup> the spectral deconvolution may have accumulated further errors, which are expected to be largest for the crowded C 1s bands of the 290–291 eV region and smallest for the comparatively simple N 1s and O 1s spectra. The comparison with the most intense profiles is reasonable because the same (i.e., ground state) geometry was assumed for the initial and final states (vertical transitions), so the calculated CEBEs likely correspond or lie close to the most intense transitions, in accordance with the Franck–Condon principle. Because it is unclear to what extent these uncertainties may contribute to errors in assessing the relative performance of the theoretical approaches if one should rely solely on the AADs, the relative overlap criterion (eq 2) for the C 1s spectra is also defined and used. The latter unbiased measure of agreement should be the preferred one because it is affected neither by the errors in the absolute vertical CEBEs nor by the possibly erroneous relative

**Table 3. Relative Overlaps (C 1s Spectra) and Average Absolute Deviations (N 1s and O 1s Spectra) for Scalar Relativistic Corrected and Original Uncorrected (In Parentheses) Core Electron Binding Energies<sup>a</sup>**

C 1s	HF		MP2		B3LYP	
	U	RO	U	RO <sup>b</sup>	U	RO
	$\Omega_{\text{rel}}$					
tempo	0.77 (0.67)	0.85 (0.89)	0.72 (0.81)	0.65 (0.73)	0.87 (0.77)	0.88 (0.88)
nitroxyl8	0.81 (0.83)	0.70 (0.75)	0.67 (0.72)	0.67 (0.72)	0.84 (0.87)	0.82 (0.88)
nitroxyl9	0.81 (0.76)	0.67 (0.75)	0.64 (0.70)	0.62 (0.68)	0.89 (0.85)	0.85 (0.89)
	AAD					
N 1s + O 1s	0.67 (0.93)	0.59 (0.79)	0.64 (0.46)	0.64 (0.37)	0.41 (0.68)	0.30 (0.53)

<sup>a</sup>The assumed relativistic corrections are 0.10, 0.21, and 0.36 eV for C, N, and O atoms, respectively.<sup>8b</sup> The wCV mixed basis set is used. <sup>b</sup>The restricted open  $\Delta$ RMP/wCV method is considered.

assignments (intramolecular chemical shifts). Occasional poorer correlation between the AAD and  $\Omega_{\text{rel}}$  value therefore indicates a significantly different performance for the C 1s, and N 1s and O 1s spectra as is, e.g., the case with the  $\Delta$ RMP/wCV method (Table 1).

The relativistic corrections to the core-electron energies, which invariably raise the calculated CEBEs, need to be considered for a more complete assessment of the relative performance of the tested methods. Estimates based on the HF/6-31G\* level and Douglas–Kroll–Hess Hamiltonian call for addition of 0.10, 0.21, and 0.36 eV for C, N, and O atoms, respectively,<sup>8b</sup> although these corrections may be different for the correlated methods.<sup>31</sup> Importantly, however, previous estimate of the relativistic increase in CEBE for the C atoms is smaller, around 0.05 eV.<sup>32</sup> Interestingly, recent corrections relying on the infinite two-component relativistic theory formalism resulted in an almost uniform increase in the  $\Delta$ MP2 CEBEs of cytosine by  $\sim 0.2$  eV, equally for the C, N, and O atoms.<sup>30</sup>

Table 3 summarizes the effects of the recently proposed scalar relativistic corrections (0.10, 0.21, and 0.36 eV for C, N, and O, respectively<sup>8b</sup>) on the relative overlaps (for the C 1s spectra) and average absolute deviations (for the combined N 1s and O 1s spectra). The least affected are the two  $\Delta$ DFT methods, whereupon introducing the corrections  $\Delta$ U-B3LYP and  $\Delta$ RO-B3LYP become comparably accurate for the C 1s spectra, and both considerably improved for the N 1s and O 1s spectra. The worst affected are the U and RO  $\Delta$ MP2 approaches, in which case the corrections further expose the problem of the generally overshoot CEBEs reducing the agreement for the C 1s, and in particular for the N 1s and O 1s spectra. Conversely, the unrestricted  $\Delta$ HF results mostly benefit nicely from the corrections, while for the N 1s and O 1s CEBEs the corrected  $\Delta$ ROHF is seen to perform better than either of the  $\Delta$ MP2 approaches (Table 3). This indicates that the extra effort to obtain the  $\Delta$ MP2 values is generally unwarranted.

Overall, the most consistent and reliable performance is offered by the  $\Delta$ RO-B3LYP/wCV method (Tables 1, 2, and 3). The relative overlaps for the C 1s spectra are in all cases very close to the exceptional 0.90. The performance of  $\Delta$ RO-B3LYP/wCV for the comparatively large and difficult free radical species is comparable to that seen previously for the closed shell molecules.<sup>8</sup> However, it is currently also demonstrated that for  $\Delta$ DFT the more economical mixed basis sets are as applicable and reliable as an extensive uncontracted basis set used on all atoms.<sup>8</sup> Similarly remarkable performance for the C 1s spectra is seen with the  $\Delta$ U-B3LYP/wCV method, especially on introducing the relativistic upshifts

(Table 3), although  $\Delta$ RO-B3LYP/wCV remains appreciably better for the N 1s and O 1s spectra. Unfortunately, the rather vexing trade-off for this gain in accuracy is the cumbersome convergence that especially plagues the best overall  $\Delta$ RO-B3LYP approach, which at times becomes the most expensive in showing a much more difficult convergence not just compared to  $\Delta$ U-DFT but also to  $\Delta$ ROHF.

Unexpectedly, the performance of  $\Delta$ RMP and  $\Delta$ UMP2 turns out disappointing considering the relative sophistication of all the tested methods. Thus, currently a worthwhile improvement over the underlying  $\Delta$ HF approaches is not observed. Quite the opposite, in most cases the second-order correction worsens the  $\Omega_{\text{rel}}$  values achieved by the reference  $\Delta$ HF approaches leading in general to the most overshoot set of C 1s CEBEs, especially for the 290–292 eV region. In addition, the relativistic corrections considerably worsen the originally encouraging agreement for the N 1s and O 1s spectra (Table 3). We conclude that it is only on rare and unpredictable occasions that the second-order approaches may warrant the additional computational effort. The performance of the original  $\Delta$ RMP/CV variant appears poorer still, while  $\Delta$ ZAPT/CV is utterly unsuitable for the prediction of CEBEs (section IIIB).

The cancellation of a good part of the correlation between the ground state and core hole cation fortuitously results in the surprisingly good performance of the  $\Delta$ HF approaches. Conversely, the overestimation of the correlation, as is common with the second-order perturbation treatments, renders especially the comparison between species with unequal number of electrons problematic. The consequent excessive lowering of the ground relative to the singly ionized state results in the systematically exaggerated CEBEs. However, as opposed to the absolute CEBEs, the chemical shifts appear to benefit more from the second-order treatment of the correlation. Most notably, the  $\Delta$ RMP/wCV ordering of CEBEs of the N atoms in nitroxyl8 and nitroxyl9 is the reverse of  $\Delta$ ROHF (Table 1), which brings it in accordance with the experimental assignment.<sup>5</sup> Also interesting is the relatively poor performance of  $\Delta$ ROHF/wCV seen for the most blue-shifted C atom (C10), which  $\Delta$ RMP/wCV is able to rectify by unexpectedly lowering the corresponding  $\Delta$ ROHF/wCV value.

Several tests that consisted of increasing the basis set quality on the core-ionized atom (up to QZ and 5Z) provided a sound indication that the second-order approaches suffer primarily from the limited basis set size within the present mixed basis set framework. The most likely principal reason is only the DZP quality basis set used on the non-core-ionized centers. In contrast, the  $\Delta$ DFT and  $\Delta$ HF approaches do not exhibit a

pronounced dependency on the basis set size, and their performance with the mixed basis sets is comparable to that seen with the extensive all-electron bases used on all atoms. The most consistent of the second-order treatments,  $\Delta$ RMP, suffers from yet another serious drawback because its efficiency is much inferior to that of the DFT; namely, the RMP step, unlike the HF or DFT, scales only very modestly with the increasing number of cores.

Focusing on the relative performance of the U and RO versions of a given method, it is seen that the two perform similarly after the relativistic corrections are taken into account (Table 3). Overall, the U methods are to some extent preferable for the C 1s, and their RO counterparts for the N 1s and O 1s spectra. In fact, a striking correlation is seen between the  $\Delta$ RO-B3LYP and  $\Delta$ U-B3LYP predictions, with the majority of the  $\Delta$ RO-B3LYP C 1s CEBEs being evenly blue-shifted by 0.12–0.13 eV and O 1s CEBEs by 0.15–0.16 eV. The notable exceptions are the two amide C atoms (C10 in nitroxyl8 and nitroxyl9), which are the only ones red-shifted by  $\Delta$ RO-B3LYP, which brings it into better agreement with the experimental CEBEs. The correlation between the  $\Delta$ UHF/ $\Delta$ ROHF and  $\Delta$ UMP2/ $\Delta$ RMP pairs of methods is more erratic. The reason for the similar performance of the U and RO methods is at most only a moderate amount of spin contamination present, which does not harm the U approaches significantly. The largest  $\langle \hat{S}^2 \rangle$  values in the UHF references are observed in nitroxyl9, and amount to 2.29 in the core-ionized state (C3), and 0.80 in the ground state (the CV basis set on N1). At times this does affect the U-SCF convergence rate although it regularly remains better than that of the RO counterparts. As is customary, the spin contamination in U-B3LYP is much smaller, at most 0.76 in ground and 2.02 in core-ionized states, although special diagnostics more appropriate for U-DFT should yield somewhat larger values.<sup>33</sup>

A finer theoretical assignment concerning the detailed C 1s chemical shifts of the C atoms within the composite bands is in principle possible given that the CEBEs faithfully echo the molecular charge distribution. A well-known formula relating the CEBE of a carbon atom A to its net partial charge  $q_A$ , the net partial charges on the remaining atoms B at the distance  $R_{AB}$ , and the relaxation energy is given by<sup>2</sup>

$$\text{CEBE}_A = kq_A + \sum_{B \neq A} \frac{q_B}{R_{AB}} + \Delta E_{\text{relax}} \quad (3)$$

where the value of  $k$  depends on the hybridization of A. The calculated CEBEs can be shown to exhibit an excellent correlation with the experiment provided a reliable set of ab initio atomic charges is plugged into eq 3 such as those proposed recently in the context of intrinsic atomic orbitals (IAO).<sup>34</sup>

For example, it is interesting to compare the CEBEs predicted for the C3 atom of nitroxyl8 and nitroxyl9. The charge is significantly depleted from C3 in nitroxyl9 due to the resonance effects involving the C3–C4 double bond conjugated to the vicinal amide, specifically the electron-withdrawing carbonyl group. Despite this, the restricted open methods invariably assign a larger CEBE to the more negative C3 of nitroxyl8, which illustrates a more pronounced sensitivity of the core orbital of the  $sp^3$  hybridized C3 atom to the inductive effects of the amide. In addition, the two positive H atoms attached to C3 of nitroxyl8 boost the second term on the RHS in eq 3 and increase the corresponding CEBE.

Analogously, the lower CEBEs of the C6 and C7 atoms of the methyl substituents relative to C8 and C9 are due to the former pair being located nearer to the amide whose N and O atoms accumulate negative charge and decrease the same term more for C6 and C7. The delocalization of charge due to the interaction between the bonding and antibonding  $\sigma(\text{C}–\text{C})$  and  $\pi(\text{N}–\text{O})$  orbitals via hyperconjugation<sup>35</sup> may account for the small relative differences in CEBEs of the two  $\text{CH}_3$  substituents attached to the same C center. The effect is most easily appreciated in tempo, where the O2–N2–C2–C10 (or O2–N2–C6–C7) and O2–N2–C2–C9 (or O2–N2–C6–C8) dihedral angles equal  $49^\circ$  and  $69^\circ$ , respectively. This renders the C8–C6 and C9–C2  $\sigma$  bonds more favorably aligned for the hyperconjugation; consequently, the C8 and C9 atoms lose more charge to the electronegative nitroxide group. Thus, the corresponding CEBEs are a sensitive indicator of the preferred conformation. Finally, an interesting interpretative problem is posed by the CEBEs of the amide C (C10) atom in nitroxyl8 and nitroxyl9. The latter compound is experimentally observed to have the larger C10 CEBE (Table 1), which indicates the more positive C10 atom. Despite this, the natural population analysis<sup>36</sup> predicts C10 of nitroxyl9 to be significantly less positive, presumably overestimating the charge transferred to it via the resonant effects involving the double bond and carbonyl group. However, the IAO charges<sup>34</sup> interestingly come out virtually equal for the two C10 atoms, which is thus more in agreement with the experimental finding.

**B. Failure of the  $\Delta$ ZAPT Approach.** Presently, a most striking methodological finding is that the  $\Delta$ ZAPT/CV approach to calculating CEBEs is highly unreliable and should be altogether avoided. This point is illustrated by the  $\Delta$ ZAPT CEBEs obtained for the C8 and C9 atoms of nitroxyl9 (Table 1). In addition, prior to the amendments described below, several more suspicious values were obtained: 278.44 eV for C8 and 390.97 eV for N2 in nitroxyl8, and 286.31 eV for C10 in nitroxyl9. All of these CEBEs turn out not only grossly underestimated but also far off from the corresponding reasonable  $\Delta$ ROHF values. Whenever possible the rectified values are given in Table 1. Significantly, the  $\Delta$ RMP results based on the identical ROHF references are all reasonable. Pointing out similar deficiencies is of interest because the past two decades of research have established ZAPT as the most successful of the perturbation theories based on a ROHF reference wave function.<sup>14,16</sup> In the following, we find that the reasons for the failure of  $\Delta$ ZAPT are essentially two, the first of which can be partially rectified, while the second is intrinsic to the ZAPT formalism.

In three cases, C8 and N2 in nitroxyl8 and C10 in nitroxyl9, the failure was found to be due to the erroneously calculated ZAPT energy of the corresponding core hole states, which is a consequence of the Aufbau violation brought on by the recanonicalization of the converged ROHF orbitals in order to prepare them for ZAPT. Namely, the default ROHF scheme in GAMESS-US produces the orbitals based on the Roothaan single matrix (RSM) canonicalization parameters,<sup>37</sup> and only subsequently do these orbitals undergo the Guest–Saunders (G-S) canonicalization<sup>38</sup> appropriate for ZAPT. The ROHF canonicalization schemes are defined through the choice of the so-called canonicalization parameters commonly denoted by  $A_{cc}$ ,  $B_{cc}$ ,  $A_{oo}$ ,  $B_{oo}$ ,  $A_{vv}$ , and  $B_{vv}$ .<sup>39</sup> These parameters multiply the standard  $\alpha$  and  $\beta$  Fock matrices, and the resulting linear combinations are used to construct the diagonal closed–closed (cc), open–open (oo), and virtual–virtual (vv) blocks of the



total ROHF Fock matrix. In the RSM canonicalization these parameters respectively equal  $-0.5$ ,  $1.5$ ,  $0.5$ ,  $0.5$ ,  $1.5$ , and  $-0.5$ , while in the G-S canonicalization they are all equated to  $0.5$ .

The Aufbau violation is usually caused by only one of the positive energy orbitals entering the occupied space and forcing out the correct negative energy orbital to the virtual space. Whenever this occurs, the ZAPT energies were found to be reparable by adopting a nonstandard procedure which consists of imposing the G-S canonicalization (in lieu of the RSM canonicalization) right from the beginning of the ROHF SCF process. In the three cases where such a procedure was found to be capable of resolving the issue, the thus rectified CEBE values are now reasonable (Table 1). In two cases (C8 of nitroxyl8 and C10 of nitroxyl9) imposing the G-S canonicalization from the beginning results in the final ROHF energies that are identical to those obtained with the RSM canonicalization. The resulting symmetrical orbitals are also identical but are this time ordered correctly by energy. In the remaining case (N2 of nitroxyl8) the ROHF energy obtained with the RSM canonicalization could not be reproduced with the G-S canonicalization, which illustrates the existence of close-lying ROHF solutions capable of adversely affecting the convergence rate.

Similar occurrences received attention recently and concerned the erroneous ordering of orbital energies in high-spin ROHF and the corresponding problems in MBPT2 potential energy surfaces observed in some theoretically difficult cases.<sup>39</sup> However, the herein described issues are different in two key respects. First, the proposed solution to avoid the orbital flipping and consequent Aufbau violation<sup>39</sup> does not apply precisely in the present case where it remains mandatory to both restrict the orbital interchanges and to resort to the DIIS to preserve the core hole configuration. Second, the problems in that study were observed equally for ZAPT and RMP,<sup>39</sup> whereas presently the  $\Delta$ RMP approach, entirely unlike the  $\Delta$ ZAPT, performs reasonably at all times.

More critical are the cases of the C8 and C9 atoms of nitroxyl9 (Table 1), where the described procedure cannot rectify the issue. These cases differ from the above because here no Aufbau violation is committed, and therefore the converged density does not differ from the Fock matrix predicted density. In fact, they constitute a clear illustration of the breakdown of the second-order perturbation approach for core hole reference wave functions. The analysis of the contributions to the ZAPT energy indicates that common to the incorrigible errors is the grossly overestimated “singly unoccupied term” in the core hole cation:<sup>14b</sup>

$$E_{\text{SU}} = \sum_{ijsb} \frac{v_{ij}^{sb}(2v_{ij}^{sb} - v_{ji}^{sb})}{\epsilon_i + \epsilon_j - \epsilon_s^- - \epsilon_b} \quad (4)$$

where the  $(i, j, \dots)$ ,  $(s, t, \dots)$ , and  $(a, b, \dots)$  sets of indices refer to the doubly occupied, singly occupied, and unoccupied symmetric spin orbitals, and  $v_{mn}^{pq}$  denotes the  $(mp|nq)$  two-electron integral in Mulliken notation. Conversely, the errors due to the overestimated “closed shell term”,<sup>14b</sup>

$$E_{\text{CST}} = \sum_{ijab} \frac{v_{ij}^{ab}(2v_{ij}^{ab} - v_{ji}^{ab})}{\epsilon_i + \epsilon_j - \epsilon_a - \epsilon_b} \quad (5)$$

i.e., the one not involving the singly occupied orbitals, are the fingerprint of the Aufbau violation and are corrigible provided

the Guest–Saunders canonicalization is imposed from the beginning.

A close look into the singly unoccupied contributions reveals that the intrinsic failures of ZAPT are in all cases due to *only one* excessively large negative contribution to the second-order energy of a given core hole state. Responsible for the large size of this contribution is a relatively large numerator coincident with a very small denominator (eq 4). This contribution involves twice the doubly occupied  $2s$  orbital, the singly occupied  $1s$  core orbital, and the orbital best described as its lowest lying virtual partner, the “ $1s^*$  orbital”. While the precise size of the contribution will be dependent on the type of the all-electron basis set used on the core-ionized atom, principally because of the variations in the energy of the virtual  $1s^*$  orbital, this is nevertheless expected to remain unphysically large.

The persistently large size of this contribution can be rationalized as follows. The spatial extensions of the core  $1s$  and inner valence  $2s$  orbitals, the former being inert and the latter participating comparatively weakly in chemical bonding, remain largely unchanged and thus comparable regardless of the system. The same holds for the  $1s^*$  orbital. Hence the  $(2s1s|2s1s^*)$  integrals in the numerator are expected not to vary much despite possibly largely dissimilar systems; in any case they retain the same order of magnitude. For example, the numerators equal  $1.3 \times 10^{-4}$  and  $2.8 \times 10^{-4} \text{ au}^2$  for  $\text{CO}_2$  and the C8 atom of nitroxyl9, respectively. Because each of the four orbitals is localized on the same center, such a numerator is also always comparatively large.

The second reason for the ZAPT breakdown is the simultaneously very small denominator. Similarly to the numerator, its persistence is due to only small variations in the  $\epsilon_{1s}$ ,  $\epsilon_{2s}$ , and  $\epsilon_{1s^*}$  energies regardless of the system. The key ingredient, however, is the energy shift, which the singly occupied orbitals undergo due to the  $Z$ -averaging inherent to the ZAPT framework. This shift is essentially constant and significantly larger for the singly occupied core than for the singly occupied valence orbitals. The examination of the Fock matrix elements in the symmetric spin–orbital basis reveals that the energy gap due to the shift is given by the sum of the two-electron integrals:<sup>14a</sup>

$$\Delta = |e^+ - e^-| = \left| \sum_t v_{ss}^{tt} \right| \quad (6)$$

where the sum goes over all the singly occupied orbitals. In the case of the core hole states the dominant contribution is due to the  $(1s1s|1s1s)$  integral, which is virtually identical for a given core-ionized atom regardless of the system. Thus, what is only a small gap in case of the typically delocalized singly occupied valence orbital (in our case this is the  $\pi^*(\text{N}-\text{O})$  orbital), becomes a much larger gap in the case of the singly occupied core orbital because of the high compactness of the latter. In the case of the three radicals and C core holes the former gap amounts to  $\sim 0.6 \text{ au}$  and the latter to  $\sim 3.6 \text{ au}$ . In a typical case of failure (C8 of nitroxyl9) the denominator comes out as small as  $0.00071 \text{ au}$ ; consequently, the corresponding contribution is 3–4 orders of magnitude larger than the second largest contribution to the “singly unoccupied term”. The small oscillations in the denominator prevent the perceptible collapse of ZAPT in every case. Therefore, the instances at which this unphysically large contribution will lead to the catastrophic breakdown of the second-order approach are unpredictable. It is thus largely by accident that  $\Delta$ ZAPT/CV performs reasonably for all C atoms of nitroxyl8, with the

only two problematic CEBEs (C8 and N2) more or less successfully rectified by imposing the G-S canonicalization from the beginning.

The described issues can be prevented by avoiding the Z-averaging and the consequent splitting of the singly occupied levels to  $\varepsilon^+$  and  $\varepsilon^-$ , which is most easily achieved by switching to the OPT1 method of Murray and Davidson.<sup>40</sup> This method uses the same orbital canonicalization scheme as ZAPT does but in place of the  $\varepsilon^+$  and  $\varepsilon^-$  energies keeps the common energy, which is the average of  $\varepsilon^+$  and  $\varepsilon^-$ .<sup>14b</sup> For analogous reasons the contribution ceases to be problematic with  $\Delta$ RMP. The comparative advantages of  $\Delta$ ZAPT, viz., avoiding different orbitals for different spins and efficient parallelization, are also retained in the  $\Delta$ OPT1 approach. However, in several cases the poor performance of  $\Delta$ ZAPT relative to  $\Delta$ RMP, such as for the N and O atoms of tempo (Table 1), could not be rectified by resorting to the  $\Delta$ OPT1; therefore, this appears to be inherent to second-order treatments relying on the symmetric spin-orbitals. An alternative solution is to altogether disallow the excitations into the singly occupied core orbital (while keeping the excitations out of this orbital). Whereas the majority of the thus excluded terms is of minor importance due to the large denominators, some of them actually contribute to lowering of the second-order energy of the core hole state. Consequently, excluding them would mostly exacerbate the problem with the overshoot CEBEs uniformly seen with the  $\Delta$ MP2 approaches.

#### IV. CONCLUSION

Within the recently proposed mixed (all-electron/core potential) basis set framework,<sup>12</sup> we have compared the performance of restricted open shell and unrestricted second-order perturbation and hybrid density functional approaches to calculating core electron binding energies. The methods were tested for the comparatively large ground state free radical species that find considerable practical use, viz., tempo and its two analogues. Two mixed basis sets were tested, the original CV<sup>12</sup> as well as the variant relying on the weighted version of the core-valence correlation set (wCV) on the core-ionized atom. The use of the latter was seen to be very beneficial for the approaches based on the second-order perturbation theories, while the difference was found to be largely immaterial in the case of the  $\Delta$ HF and  $\Delta$ DFT approaches.

Two criteria for assessing the relative performance were adopted. Because the standard criterion of average absolute deviations suffers from larger uncertainties in the experimental assignments than those typically seen in less complex systems,<sup>5</sup> the criterion of overlap between the experimental and modeled C 1s spectral curves was also introduced. The best performance according to both criteria is offered by the  $\Delta$ RO-B3LYP/wCV method. On the other hand, the second-order perturbation  $\Delta$ RMP,  $\Delta$ ZAPT, and  $\Delta$ UMP2 approaches exhibited a surprisingly poor performance and for the most part did not warrant the additional computational effort over the underlying  $\Delta$ HF treatments. The most worrisome issue with the second-order approaches is in systematically overestimated CEBEs, which consequently deteriorate even more on including the relativistic corrections. By far the poorest performance is seen with the  $\Delta$ ZAPT/CV approach, which suffered several grave failures that completely devalue its applicability for calculating CEBEs. These failures are the consequence of the breakdown of the second-order perturbation approach due to only one unphysically large contribution to the ZAPT energy, specifically

caused by the shift in the energy undergone by the singly occupied orbitals inherent to the ZAPT formalism.

For modeling the core-ionized spectra of free radicals, applying restricted open shell formalisms provides some improvement in accuracy over the corresponding unrestricted formalisms. However, this comes at the expense of a more cumbersome convergence for the core hole states even though such a difficult convergence is normally not encountered in smaller systems.

Overall, the unrestricted and restricted open  $\Delta$ DFT approaches in conjunction with the mixed basis sets represent an accurate and efficient route to calculating core-ionization energies of free radicals. Apart from effectively solving the problem of the clear-cut localization of core hole, the mixed basis sets appear capable of achieving the accuracy comparable to that seen with the extensive all-electron basis sets<sup>8</sup> while simultaneously being more economical due to the omission of the core shells on the noncore ionized atoms. The latter aspect allows for a more efficient treatment of larger systems especially if heavier atoms are involved. Finally, in light of the recent extensive tests of the  $\Delta$ DFT methods,<sup>18</sup> the performance of some other hybrid functionals for the free radicals could turn out to be better still than the presently used B3LYP.

#### AUTHOR INFORMATION

##### Corresponding Author

\*E-mail: iljubic@irb.hr.

##### Funding

Financial support from the Croatian Ministry of Science, Education and Sport under Project No. 098-0982915-2944 is acknowledged.

##### Notes

The authors declare no competing financial interest.

#### ACKNOWLEDGMENTS

I am much indebted to Dr. Branka Kovač for numerous valuable discussions and for providing the XPS spectra.

#### REFERENCES

- (1) Fadley, C. S. *J. Electron Spectrosc. Relat. Phenom.* **2010**, 178–179, 2–32.
- (2) (a) Siegbahn, K.; Nordling, C.; Johansson, G.; Hedman, J.; Heden, P.-F.; Hamrin, K.; Gelius, U.; Bergmark, T.; Werme, L. O.; Manne, R.; Baer, Y. *ESCA Applied to Free Molecules*; North-Holland: Amsterdam, The Netherlands, 1969. (b) Barr, T. L. *Modern ESCA: The Principles and Practice of X-ray Photoelectron Spectroscopy*; CRC Press: Boca Raton, FL, USA, 1994.
- (3) Osborne, S. J.; Sundin, S.; Ausmees, A.; Svensson, S.; Saethre, L. J.; Svaeren, O.; Sorensen, S. L.; Vêgh, J.; Karvonen, J.; Aksela, S.; Kikas, A. *J. Chem. Phys.* **1997**, 106, 1661–1668.
- (4) Novak, I.; Harrison, L. J.; Kovač, B.; Pratt, L. M. *J. Org. Chem.* **2004**, 69, 7628–7634.
- (5) Kovač, B.; Ljubić, I.; Kivimäki, A.; Coreno, M.; Novak, I. *Phys. Chem. Chem. Phys.* **2014**, 16, 10734–10742.
- (6) (a) Krishna, M. C.; Grahame, D. A.; Samuni, A.; Mitchell, J. B.; Russo, A. *Proc. Natl. Acad. Sci. U. S. A.* **1992**, 89, 5537–5541. (b) Galli, C. Nitroxyl Radicals. In *The Chemistry of Hydroxylamines, Oximes and Hydroxamic Acids*, Vol. 1; Rappoport, Z., Liebman, J. F., Eds.; John Wiley & Sons: Chichester, U.K., 2008; pp 705–750.
- (7) Naves de Brito, A.; Correia, N.; Svensson, S.; Ågren, H. *J. Chem. Phys.* **1991**, 95, 2965–2974.
- (8) (a) Gilbert, A. T. B.; Besley, N. A.; Gill, P. M. W. *J. Phys. Chem. A* **2008**, 112, 13164–13171. (b) Besley, N. A.; Gilbert, A. T. B.; Gill, P. M. W. *J. Chem. Phys.* **2009**, 130, No. 124308.

- (9) Bagus, P. S.; Schaefer, H. F., III. *J. Chem. Phys.* **1972**, *56*, 224–226.
- (10) (a) Takahata, Y.; Chong, D. P. *J. Electron Spectrosc. Relat. Phenom.* **2003**, *133*, 69–76. (b) Chong, D. P. *J. Electron Spectrosc. Relat. Phenom.* **2007**, *159*, 94–96.
- (11) Holme, A.; Børve, K. J.; Sæthre, L. J.; Thomas, T. D. *J. Chem. Theory Comput.* **2011**, *7*, 4104–4114.
- (12) (a) Shim, J.; Klobukowski, M.; Barysz, M.; Leszczynski, J. *Phys. Chem. Chem. Phys.* **2011**, *13*, 5703–5711. (b) Fitzsimmons, A.; Klobukowski, M. *Theor. Chem. Acc.* **2013**, *132*, 1314.
- (13) (a) Knowles, P. J.; Andrews, J. S.; Amos, R. D.; Handy, N. C.; Pople, J. A. *Chem. Phys. Lett.* **1991**, *186*, 130–136. (b) Lauderdale, W. J.; Stanton, J. F.; Gauss, J.; Watts, J. D.; Bartlett, R. J. *Chem. Phys. Lett.* **1991**, *187*, 21–28.
- (14) (a) Lee, T. J.; Jayatilaka, D. *Chem. Phys. Lett.* **1993**, *201*, 1–10. (b) Lee, T. J.; Rendell, A. P.; Dyall, K. G.; Jayatilaka, D. *J. Chem. Phys.* **1994**, *100*, 7400–7409.
- (15) Jayatilaka, D.; Lee, T. J. *Chem. Phys. Lett.* **1992**, *199*, 211–219.
- (16) Wheeler, S. E.; Allen, W. D.; Schaefer, H. F., III. *J. Chem. Phys.* **2008**, *128*, No. 074107.
- (17) Besley, N. A.; Asmuruf, F. A. *Phys. Chem. Chem. Phys.* **2010**, *12*, 12024–12039.
- (18) Tolbatov, I.; Chipman, D. M. *Theor. Chem. Acc.* **2014**, *133*, 1473.
- (19) Gill, P. M. W.; Pople, J. A.; Radom, L.; Nobes, R. H. *J. Chem. Phys.* **1988**, *89*, 7307–7314.
- (20) Woon, D. E.; Dunning, T. H., Jr. *J. Chem. Phys.* **1995**, *103*, 4572–4585.
- (21) Peterson, K. A.; Dunning, T. H., Jr. *J. Chem. Phys.* **2002**, *117*, 10548–10560.
- (22) Miyoshi, E.; Mori, H.; Hirayama, R.; Osanai, Y.; Noro, T.; Honda, H.; Klobukowski, M. *J. Chem. Phys.* **2005**, *122*, No. 074104.
- (23) Dunning, T. H., Jr. *J. Chem. Phys.* **1989**, *90*, 1007–1023.
- (24) (a) Becke, A. D. *J. Chem. Phys.* **1993**, *98*, 5648–5642. (b) Stephens, P. J.; Devlin, F. J.; Chablowski, C. F.; Frisch, M. J. *J. Phys. Chem.* **1994**, *98*, 11623–11627.
- (25) Schmidt, M. W.; Baldridge, K. K.; Boatz, J. A.; Elbert, S. T.; Gordon, M. S.; Jensen, J. J.; Koseki, S.; Matsunaga, N.; Nguyen, K. A.; Su, S.; Windus, T. L.; Dupuis, M.; Montgomery, J. A. *J. Comput. Chem.* **1993**, *14*, 1347–1363.
- (26) Vosko, S. H.; Wilk, L.; Nusair, M. *Can. J. Phys.* **1980**, *58*, 1200–1211.
- (27) Pulay, P. *J. Comput. Chem.* **1982**, *3*, 556–560.
- (28) Giffin, N. A.; Makramalla, M.; Hendsbee, A. D.; Robertson, K. N.; Sherren, C.; Pye, C. C.; Masuda, J. D.; Clyburne, J. A. C. *Org. Biomol. Chem.* **2011**, *9*, 3672–3680.
- (29) Fairlie, D. P.; Woon, T. C.; Wickramasinghe, W. A.; Willis, A. C. *Inorg. Chem.* **1994**, *33*, 6425–6428.
- (30) Barysz, M.; Klobukowski, M.; Leszczynski, J. *Struct. Chem.* **2012**, *23*, 1293–1299.
- (31) Klopper, W. *J. Comput. Chem.* **1997**, *18*, 20–27.
- (32) Chong, D. P. *J. Chem. Phys.* **1995**, *103*, 1842–1845.
- (33) Cohen, A. J.; Tozer, D. J.; Handy, N. C. *J. Chem. Phys.* **2007**, *126*, 214104.
- (34) Knizia, G. *J. Chem. Theory Comput.* **2013**, *9*, 4834–4843.
- (35) Alabugin, I. V.; Gilmore, K. M.; Peterson, P. W. *WIREs Comput. Mol. Sci.* **2011**, *1*, 109–141.
- (36) Reed, A. E.; Weinstock, R. B.; Weinhold, F. *J. Chem. Phys.* **1985**, *83*, 735–746.
- (37) Roothaan, C. C. J. *Rev. Mod. Phys.* **1960**, *32*, 179–185.
- (38) Guest, M. F.; Saunders, V. R. *Mol. Phys.* **1974**, *28*, 819–828.
- (39) Glaesemann, K. R.; Schmidt, M. W. *J. Phys. Chem. A* **2010**, *144*, 8772–8777.
- (40) Murray, C.; Davidson, E. R. *Chem. Phys. Lett.* **1991**, *187*, 451–454.